PHILOSOPHICAL TRANSACTIONS OF THE ROYAL SOCIETY A MATHEMATICAL, PHYSICAL & ENGINEERING SCIENCES

Echoes and Imaging in Solids [and Discussion]

J. H. Strange, P. Mansfield, M. Wormald, W. Derbyshire and E. R. Andrew

Phil. Trans. R. Soc. Lond. A 1990 **333**, 427-439
doi: 10.1098/rsta.1990.0170

Echoes and imaging in solids

By J. H. Strange

Physics Laboratory, The University, Canterbury, Kent CT2 7NR, U.K.

The broad spectral lines usually encountered in solid state NMR present considerable difficulties for imaging. One successful approach to the problem is to artificially narrow the line by multipulse or sample spinning methods. An alternative is to apply sufficiently large magnetic field gradients that they dominate the line broadening and seek ways to deal with bandwidth and power requirements thereby introduced. This paper explores the second route and demonstrates that spin-echo techniques help to solve several of the inherent problems. Gradient echoes produced by periodic reversal of the field gradients have significant advantages. The addition of synchronous RF pulses can produce an extended train of 'solid' echoes which overcomes, at least to some extent, the bandwidth limitation of this approach and permits rapid imaging in two dimensions. Slice selection and three-dimensional back-projection have also been achieved in solid-like samples. Comparison with line-narrowing methods and relative advantages of the different approaches are addressed.

1. Introduction

In solids, or solid-like material where atomic motion is very restricted, the nuclear magnetic resonance (NMR) lines are broad and transverse relaxation times, T_2, are characteristically short compared with those normally found in liquids. This presents a very severe problem for the application of imaging techniques to such materials. A simple comparison of conventional methods applied to a liquid with T_2 of 100 ms and a solid with T_2 of 100 μs shows that field gradients for the latter must be 1000 times greater and the apparatus bandwidth must be increased by a similar factor to achieve comparable spatial localization. Signal-to-noise ratios will be reduced by the square root of the bandwidth ratio, i.e one to two orders of magnitude. This illustrates the fundamental problem as well as indicating the technical difficulties of dealing with a much shortened timescale. If the spin-lattice relaxation time, T_1, is also reduced in the same ratio as T_2, however, the signal-to-noise problem is much less severe since repetitative signal averaging can produce a similar noise reduction to narrowing the receiver bandwidth. Characteristically, however, solids have T_1s that are several orders of magnitude larger than T_2.

To achieve imaging sensitivity and resolution comparable with that obtainable for liquid-like objects it is necessary to preserve the transverse magnetization for times approaching T_1. This can be achieved with varying degrees of success, by special radio-frequency (RF) irradiation methods as discussed later or by physically spinning the sample at the magic angle (Cory *et al.* 1988). The mechanisms responsible for the broadened NMR lines in solids arise from various sources. The most common dominant mechanism with abundant nuclei is the direct homonuclear dipolar

Phil. Trans. R. Soc. Lond. A (1990) **333**, 427–439
Printed in Great Britain

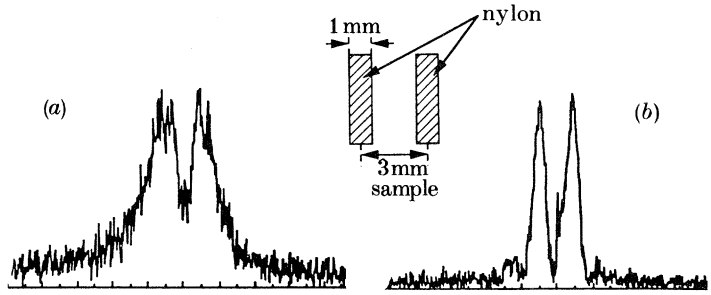

Figure 1. One-dimensional projection of the nylon phantom obtained by Fourier transformation of the (*a*) free induction decay and (*b*) spin echo as described in the text.

interaction. This produces a homogeneous broadening. In addition, heteronuclear, nuclear electric quadrupole, chemical shift and susceptibility broadening can be significant. It is therefore necessary to consider the removal of homogeneous and inhomogeneous broadening mechanisms. There are basically two approaches to the RF pulse method of extending the apparent T_2 to improve wide-line imaging.

One approach is to artificially reduce the transverse relaxation using, for example, the techniques used for high-resolution NMR in solids. One of the first ever reports of a magnetic resonance imaging experiment was by Mansfield & Grannell (1973, 1975), who used a multipulse line-narrowing sequence combined with a magnetic field gradient to produce spatial information in a solid sample. The pulse sequence was designed to reduce both dipolar and anisotropic chemical shift interactions but preserve that of the magnetic field gradient. It was noted in this earliest paper that the efficiency of line-narrowing was reduced when the field was set off-resonance so that there was a limit to the magnitude of the applied field gradient that could be tolerated if adequate line-narrowing were to be achieved. There was a long period before further substantial developments in the imaging of solids were reported with only one new approach reported within the next ten years (Wind & Yannoni 1979), again using multipulse line narrowing. This work exploited the field off-set sensitivity of the multipulse sequences. The first successful two-dimensional images of solids were reported by Chingas *et al.* (1986) using a multipulse method. These methods have since been developed to a level where proton imaging in small solid objects can be achieved in two dimensions with a resolution of better than 100 μm (Cory *et al.* 1990; Garroway, this symposium). A substantial advance in solid state imaging methods occurred with the introduction of oscillating field gradient techniques (Cottrell *et al.* 1989; Miller & Garroway 1989). These sequences are capable of removing inhomogeneous as well as homogeneous broadening interactions which is a feature that assumes increasing importance the higher the Larmor frequency that is used.

The alternative strategy to line narrowing as described is to accept the broad line width, ΔB, and impose a sufficiently large magnetic field gradient to produce spatial localization on the resonant spins. This straightforward approach was adopted by Suits & White (1984), who took account of the measured line-width in zero field gradient by using a modified projection–reconstruction algorithm in an attempt to mathematically remove the natural line width. This approach can have only limited success and depends on spectrometer sensitivity. In the same year a more sophisticated approach was adopted by Garroway *et al.* (1984), who reported a

PHILOSOPHICAL TRANSACTIONS OF THE ROYAL SOCIETY A MATHEMATICAL, PHYSICAL & ENGINEERING SCIENCES

method using multiple quantum coherence to achieve an effective field gradient which was several times larger than the actual field gradient applied. Multiple quantum transitions, of course, give weaker intensity signals than the normal resonance. Other attempts to use large static gradients have used a sensitive slice approach (Corti *et al.* 1988) and large static field gradients directly (Samoylenko *et al.* 1988). Spin-echo methods (Ibbett 1988), which have also been shown to permit slice selection (Cottrell *et al.* 1988), seem to offer the most promise with this class of method.

Let us now consider in more detail the difficulties encountered when trying to image broad-line materials by conventional imaging methods. The field gradient G required to provide a resolution Δx must be large enough to satisfy

$$G_x \Delta x \geqslant \Delta B, \tag{1}$$

where ΔB is the natural line-width of the sample. For an object of dimension x this gradient produces a transverse relaxation time that is reduced to

$$T_2^* \leqslant x^{-1} \Delta x \, T_2. \tag{2}$$

The major disadvantages with the direct approach are therefore:

(1) much of the signal is lost within the receiver dead-time following the RF excitation (90°) pulse;

(2) it is difficult to switch the large field gradients required within times short compared with T_2^*;

(3) if, to overcome (*b*), the large gradient G is established before the excitation pulse, this pulse must be very short and intense to excite the full spectral width of an object (xG_x);

(4) since T_2^* is very short, the receiver bandwidth must be broad and therefore the signal-to-noise ratio will be low.

2. Spin echo modulation

The second strategy will now be explored further and methods described that have been devised to overcome the difficulties listed above. To combat the first problem a spin echo (Hahn 1950) allows the signal to be moved beyond the receiver dead-time (Ibbett 1988). An example of the improvement in profile obtained by this simple expedient is shown in figure 1. This shows the Fourier transformation of (*a*) the free induction decay following a 90° pulse and (*b*) the spin echo following a 90°–τ–180° pulse sequence. The sample consisted of two nylon discs of 3 mm diameter, 1 mm thickness and 2 mm separation aligned with a common axis. The projection is onto the axis. Nylon has a T_2 of 40 μs, the 90° pulse was 6 μs and the receiver dead-time was 8 μs. A field gradient of 0.6 T m^{-1} was applied and the Larmor frequency for the protons was 30 MHz. The gain in peak separation and signal-to-noise ratio is clearly evident. The image quality is dependent on the pulse separation, τ, since the dead-time following the 180° pulse can obscure part of the echo signal and yet it is desirable to make τ as short as possible to maximize the echo. This example was taken with a spectrometer of only moderate specification. A high-frequency machine, with submicrosecond pulse length and a dead-time of a few microseconds would produce a much better image. The resolution is proportional to the field gradient G (equation (1)) so that power considerations provide a physical limit to the increase in gradient, particularly for large objects.

PHILOSOPHICAL TRANSACTIONS OF THE ROYAL SOCIETY A MATHEMATICAL, PHYSICAL & ENGINEERING SCIENCES

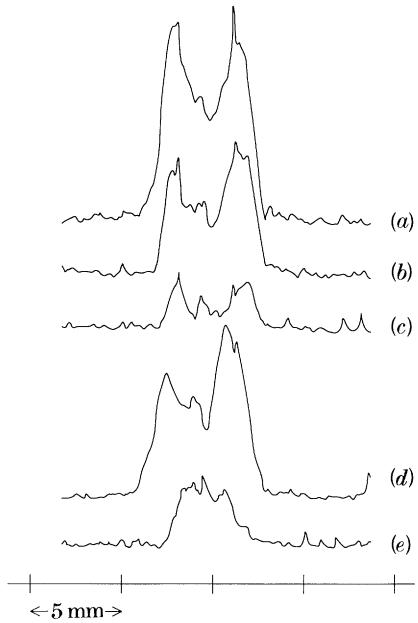

Figure 2. One-dimensional projection onto the axis of a cylinder composed of a 4 mm length of SnF_2 and 2 mm length of PbF_2 obtained by ^{19}F NMR as described in the text. Curves (*a*), (*b*) and (*c*) were before heating, (*d*) and (*e*) after heating to 200 °C. Repetition periods of the spin-echo sequence used were (*a*) 100 s, (*b*) 5 s, (*c*) 0.5 s, (*d*) 100 s, (*e*) 60 ms.

The echo method is easily adapted for T_1 mapping in solids and has been used to demonstrate that it is possible to monitor an inter-diffusional process in the solid state (Ibbett 1988). Lead fluoride, PbF_2, and tin fluoride, SnF_2, crystals both have a fluorite structure. The ^{19}F NMR signal has a T_2' at room temperature of about 35 μs in both materials and corresponds to the rigid lattice. A cylindrical sample, of diameter 4 mm and length 6 mm was made of compacted fluoride powder, with 4 mm of the length occupied by SnF_2, the remaining 2 mm by PbF_2. Using a single spin echo with $\tau = 25$ μs and $G = 1$ T m^{-1} projections of the flourine ion density were obtained along the cylindrical axis. The T_1 of the ^{19}F nuclei in SnF_2 was 20 s and in PbF_2 was 6 s at 21 °C. On heating, these materials can be sintered. The F^- becomes more mobile in the mixed halide $PbSnF_2$ with T_1 typically 50 ms at 21 °C. Examples are shown in figure 2 of one-dimensional ^{19}F images at different repetition rates for the initial sample, and after heating to 200 °C for $2\frac{1}{2}$ h. Curve (*a*) should be a simple square-shaped function but probably reflects uneven packing of the powder. Curve (*b*) shows a more significant decrease in the left side of the plot, corresponding to the longer T_1 of SnF_2. (*c*) The signal is heavily attenuated at 500 ms. (*d*) After heating, the low repetition rate signal has changed little but curve (*e*) shows a substantial signal with a short T_1 corresponding to the formation of the sintered material.

Although the spin-echo method can reduce the problem of receiver dead-time there is still the problem of producing a short 90° pulse. If RF power is inadequate only part of the object will be observed. For a sample of length x in a gradient G_x the RF field B_1 must meet the condition

$$B_1 \gg G_x x \gg \Delta B. \tag{3}$$

If this condition is not fulfilled the spatial variation of signal intensity will not only

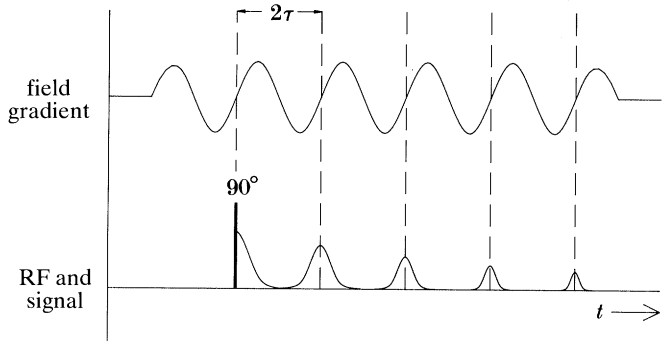

Figure 3. The timing diagram used to produce gradient echoes.

be a function of spin density but will depend on position in the field gradient. Artefacts in the spin-echo are also introduced (Ibbett 1988), which result in an oscillatory modulation of the projections produced from the echo.

It is clearly desirable to apply the RF pulses in the absence of any large magnetic field gradients and then observe the signal in the presence of a gradient. To switch large gradients reliably and allow them to settle in times short compared with the T_2 of a typical solid is difficult and is severely hampered by inductive effects although considerable progress has been made recently (Miller *et al.* 1989). To switch the gradients within T_2^*, the decay time in the presence of the large encoding gradient, is even more stringent. A reliable way to achieve a known and rapidly varying time-dependent gradient is to use sinusoidal variation. The use of such a scheme for imaging solids has been shown to have a number of advantages (Cottrell *et al.* 1990). The power requirement for the large gradients can be reduced by making the gradient coils part of a tuned circuit; the gradient can be applied with sufficient strength to dominate the homogeneous dipolar broadening; the initial 90° pulse can be applied at a zero crossing of the sinusoid, so that the RF power requirement is simply that normally associated with a solid; and no 180° pulse is required to produce the echo. The first half-cycle of the field gradient (figure 3) encodes the spatial information on the FID. The gradient is then reversed in the second half-cycle with a Hahn-type echo forming after one period of the gradient oscillation (shown at 2τ in figure 3). The echo will also contain spatial information. Provided that $2\tau < T_2$ further gradient echoes will continue to form at times $2n\tau$, the amplitudes decreasing successively as determined by T_2. A suitable choice of gradient permits the echo formation to be clear of the 90° pulse dead-time and, of course, there is no 180° pulse to further obscure the signal. It is then possible to use all of the time of the normal T_2 decay within which the echoes occur independent of the resolution demanded and gradient applied. The optimized image will be obtained by summation of the signal from each echo (assuming that T_2 does not have an important spatial variation) and a gain in signal-to-noise achieved by 'noise averaging'. Alternatively, the complete echo train may be Fourier transformed to produce an alternative projection representation of the object, although in this case the projection will consist of a series of equally spaced broadened lines similar to that obtained in echo-planar imaging (Mansfield 1977), but without the second broadening gradient. (The latter could, of course, be applied if T_2 were sufficiently long or gradients sufficiently intense.) It should be noted that echoes form when the gradient is changing most

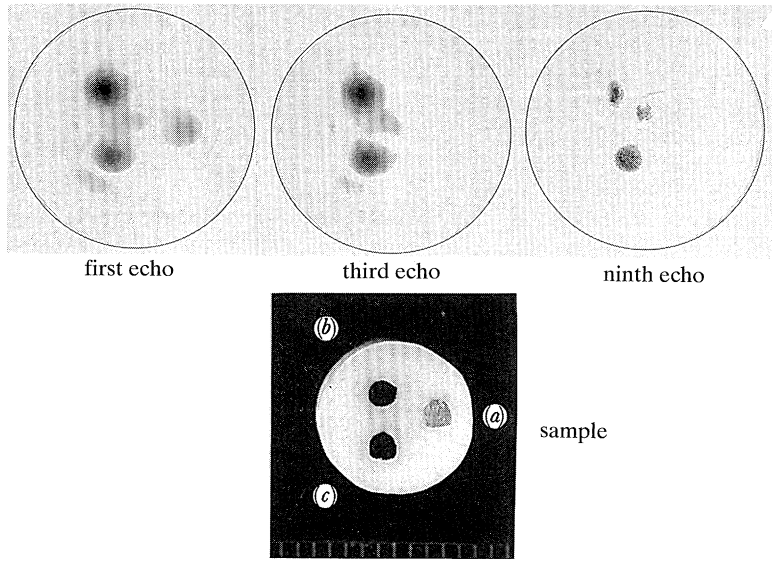

Figure 4. Image of three different rubber samples whose T_2s differ due to variation in cross-link density. Samples were 1 mm diameter, 3 mm in length. The first, third and ninth echoes occurring at $t = 170$ μs, 500 μs and 1.5 ms respectively show the decreased intensity and disappearance of the signal from the heavily cross-linked sample (a) with $T_2 = 300$ μs and the decreased intensity of sample (b) $T_2 = 750$ μs, relative to sample (c) $T_2 = 900$ μs.

rapidly and is crossing zero. This requires care in data handling and is best treated by using nonlinear sampling (Ordidge & Mansfield 1985) and phase correction for the gradient reversal at the echo maxima (Cottrell *et al.* 1990; Cottrell 1990).

The gradient spin echo or multiple spin echo sequence provides a simple means of imaging broad-line materials that could prove particularly useful for 'intermediate' broad lines such as those observed in rubbers and other soft polymers. An example of T_2 mapping, using signals from different echoes in a train of gradient echoes is shown in figure 4. The more heavily cross-linked sample ($T_2 = 300$ μs) is not seen clearly in the images formed from the later echoes. The results demonstrate the feasibility of mapping cross-link densities in rubber by MRI methods.

The remaining difficulty mentioned in (d) above rises when $T_2 \ll T_1$ so that data collection takes much longer than for liquids (where usually $T_2 \approx T_1$). Multipulse line-narrowing sequences such as MREV 8 (Mansfield 1971) have been specifically designed to extend T_2 and preserve chemical shift information. Efforts have recently been directed at modifying this type of sequence to remove inhomogeneous and homogeneous broadening while preserving the evolution of magnetization under the effect of an applied field gradient (Cottrell *et al.* 1989; Miller & Garroway 1989; McDonald & Tokarczuk 1989). Multiple-pulse methods are generally intolerant to frequency off-set and although this problem can be reduced by careful pulse sequence design, this class of method is generally appropriate for relatively weak field gradients. There is also usually a scaling down of the effective field gradient associated with the multipulse sequence so that tolerance to field off-set can be more critical than might at first appear.

The simplest pulse train that can be used to extend the transverse magnetization is the $90^\circ_x \tau (90^\circ_y 2\tau)_n$ sequence that produces a sequence of solid echoes (Mansfield &

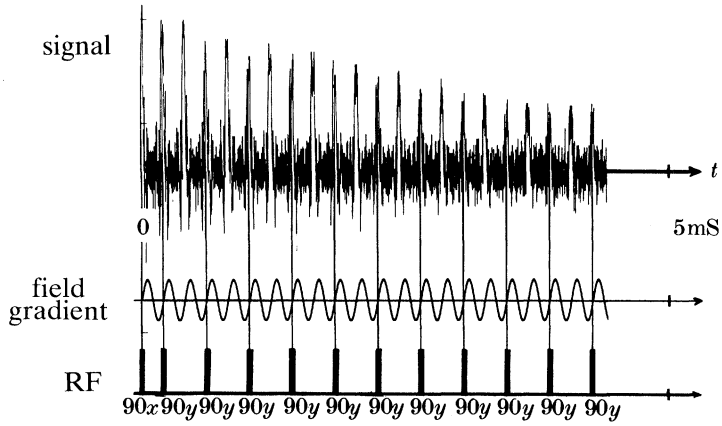

Figure 5. The timing diagram of a pulse sequence used to combine Hahn and multiple solid-echoes for imaging solids. An echo sequence obtained from a polymer sample is shown in which $T_2 = 500$ μs is extended to $T_2^+ \approx 5$ ms.

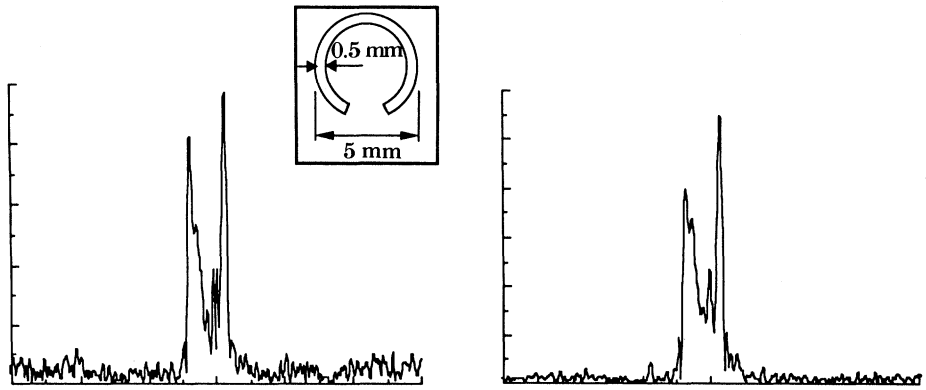

Figure 6. A proton image obtained by a gradient echo train extended by 90° pulses as shown in figure 5. The sample is a partial cylinder of cross-linked polymer (Cottrell *et al.* 1990). The projection shown on the left was obtained from a single echo; that shown on the right was obtained by summing 10 echoes.

Ware 1966; Ostroff & Waugh 1966). In the presence of the time-dependent field gradients under discussion the pulses must be applied to all nuclei with the correct phase. This requires that the 90°_y pulses are applied only at the peaks of the spin echoes. A long sequence of echoes can then be accumulated with each echo profile containing the spatially encoded information. Variations on this scheme include the application of RF pulses on alternate echoes only (figure 5) so that the other echoes are completely free from pulse interference. A one-dimensional projection obtained by summing ten echoes is shown in figure 6. Comparison with the single echo experiment shows a signal-to-noise improvement of two or three as expected.

An alternative description of the reason for the extended T_2^+ is to consider the evolution of the spins in an average RF field B_1 produced by the rapid sequence of pulses. The nuclei are effectively spin-locked along this (pulsed) resonant rotating magnetic field and the transverse magnetisation will ultimately decay with a time constant approaching $T_{1\rho}$, the spin-lattice relaxation time in the rotating frame,

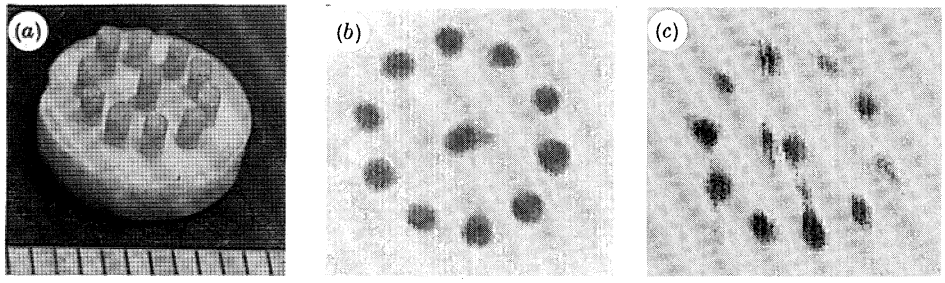

Figure 7. Proton images of the object shown (*a*) on the left were obtained by the spin-echo method (*b*) (centre) and the planar method (shown at (*c*) on the right) as described in the text.

rather than T_2. In solids, where the molecular motion is usually slower than the frequency $\omega_1 (= \gamma B_1)$ and $T_{1\rho} \propto \omega_1^2 \propto B_1^2$, increased pulse repetition frequency will increase the average B_1 and extend the transverse decay making more echoes available. The possibility of $T_{1\rho}$ mapping is evident.

It has been noted on previous occasions (Ostroff & Waugh 1966) that the Carr–Purcell Meiboom–Gill echo sequence (Meiboom & Gill 1958), which can be represented by $90^\circ_x \tau (180_y 2\tau)_n$, can be used to extend the transverse decay of a strongly dipolar coupled system, provided $2\tau < T_2$. Again, the magnetization is effectively spin-locked along the average RF field and the decay time approaches $T_{1\rho}$ for short τ values. The difficulty here is that, for imaging, the RF pulses are applied to the magnetization when the field gradient has randomized the phase of the components of transverse magnetization so that only partial spin-locking is achieved. This sequence of echoes has, however, been successfully used with a strong steady field gradient to image phantoms of adamantane, where the T_2 of 50 μs was effectively increased to 1.5 ms (Ibbett 1988). 180° pulses can also be used instead of the 90° pulses in the oscillating field gradient sequence of figure 5. This is usually found, however, to be less effective than the 90° pulse sequence in extending T_2 although 180° pulses are valuable for removing the effects of inhomogeneous broadening.

The normal method adopted in solid-state imaging to produce two-dimensional images is filtered back-projection (Brooks & Di Chiro 1973) which combines projection profiles obtained by rotating the field gradient between each sequence. An example of a two-dimensional image obtained by the spin-echo method is shown in figure 7*b*. The object consisted of a circular array of eleven solid cylinders of cross-linked rubber ($T_2 \approx 900$ μs). Each cylinder was approximately 3 mm in length and 1 mm in diameter and was mounted in a teflon former as shown in the photograph figure 7*a*). The 90° pulses were 5 μs in length and the oscillating field gradient was 2 kHz in frequency and 0.6 T m^{-1} amplitude. The resonance frequency was 21 MHz.

3. Planar imaging

The gradient echo sequence provides an opportunity to obtain images of a two-dimensional plane in a time of order T_2^+. The echo-planar method used in liquids (Mansfield 1977) would not permit the increased T_2^+ to be achieved by the simple 90° solid-echo sequence used above because of the accumulated phase shift produced in the second gradient. It could possibly be achieved with very short pulses to dephase and rephase magnetization in the second gradient direction. Planar imaging can be

PHILOSOPHICAL TRANSACTIONS OF THE ROYAL SOCIETY A MATHEMATICAL, PHYSICAL & ENGINEERING SCIENCES

achieved by another route since the gradient can be changed in direction between each echo formation so that each echo envelope provides a different projection profile. The method lacks the efficiency and elegance of the even k-space mapping possible with echo-planar imaging, but a single sequence of echoes can provide the required number of projections for the filtered back-projection reconstruction. Compensation for the echo amplitude decay, T_2^+, must be included in the data processing and any spatial variation of T_2^+ would, of course, prove to be a complicating factor. The technique has been demonstrated with the phantom object used in the previous example (Halse *et al.* 1990) and the image obtained is shown in figure 7*c*. Because the signal-to-noise was poor the picture shown is the average of 100 repeated echo sequences and was obtained in 10 s. The method will benefit from further development and could prove very valuable where time-resolved effects are to be monitored. It should be possible to follow changes in two dimensions that occur on a timescale of the order of T_1.

4. Slice selection and three-dimensional imaging

Most attention has been directed at overcoming the broad-line problems associated with two-dimensional imaging in solids. There are relatively few examples of actual two-dimensional images in the literature and the problems of obtaining satisfactory slice selection or three-dimensional image production has apparently received little attention. It is the requirement of the rapid switching of magnetic field gradients within a time T_2 that proves difficult to meet. One example of slice selection by selective excitation in a large field gradient has been demonstrated in which the magnetization is preserved by using a spin-locking technique (similar to that of Chingas *et al.* 1986) during the period required to remove the slice-selection gradient and establish the imaging gradient (Cottrell *et al.* 1988). The sequence of events is shown in figure 8. The method can be used to provide the transverse magnetization for subsequent treatment by line-narrowing or multiple echo sequences to obtain a two-dimensional image of the slice. The RF pulse amplitude B_1 is low during the application of the slice selecting magnetic field gradient G_x ($B_1 \ll G_x x$) but the spin-locking field must be larger than the gradient variation $G_y y$ over the sample during read-out and this is demanding. An alternative method is based on the slice selection method demonstrated by Wind & Yannoni (1979) in which selection is achieved by application of a large magnetic field gradient while the magnetization is spin-locked in the rotating reference frame. This has been adapted for solids imaging using the gradient echo method (Cottrell 1990). The minimum slice achieved so far is about 1 mm but increased selection gradients can reduce this substantially provided signal-to-noise ratios permit.

An alternative to slice selection, and an approach that is likely to be more efficient and desirable for materials testing, is to image in three dimensions. There is a variety of alternative approaches including Fourier imaging (Kumar *et al.* 1975), echo-planar methods (Mansfield 1977) and projection reconstruction (Lai & Lauterbur 1980). Again, for solids, the projection reconstruction method is favoured although a fairly broad-line polymeric sample has been imaged successfully in three dimensions using a 'conventional' imaging system, the Fourier transform method, but with specially constructed gradient coils (Carpenter *et al.* 1989). The projection reconstruction method has been successfully applied to cross-linked rubber ($T_2 \approx 700$ μs) using the method of pulse-sustained gradient echo modulation and three orthogonal field

PHILOSOPHICAL TRANSACTIONS OF THE ROYAL SOCIETY A MATHEMATICAL, PHYSICAL & ENGINEERING SCIENCES

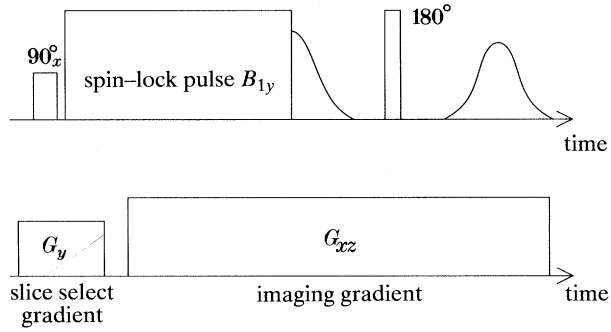

Figure 8. Slice selection timing diagram. The spin-locking pulse preserves the transverse magnetization selected by the 90° pulse while the gradient G_y is removed and G_{xy} is applied.

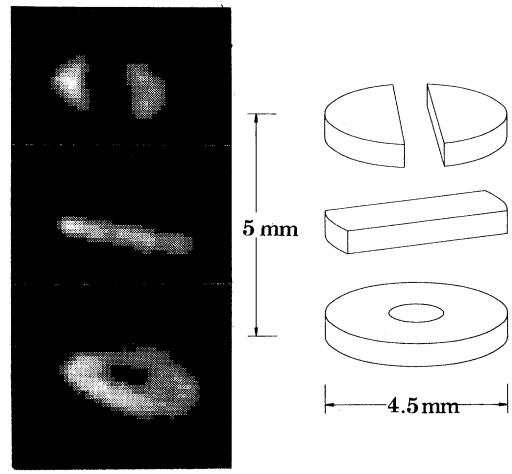

Figure 9. Cross sections obtained by proton imaging in three dimensions of the rubber object shown in the 'exploded' diagram on the right. The three sections were actually in physical contact.

gradients (Cottrell 1990; Cottrell *et al.* 1990). The phantom is shown in figure 9 together with cross-sectional images corresponding to the three major elements of the subject. The overall sample size is about 5 mm in each direction and the resolution in each is *ca.* 0.5 mm. This resolution is probably limited by the number of projections (18 × 18) taken in this case.

5. Discussion

To achieve successful NMR imaging in solids with a quality and in a time that can approach that now achieved in liquids it is necessary to extend the observation time of the transverse magnetization so that T_2^+ approaches T_1 as it does in most liquids. The attainable limit is often governed by $T_{1\rho}$ rather than T_1 in practice. It is also necessary to be able to apply field gradients to achieve the required resolution without loss of line-narrowing efficiency. The three most successful methods seem to be

(1) magic angle spinning, which is restricted to samples which have only moderate linewidth and are physically suitable for high speed rotation; synchronous rotation of the encoding gradients is also necessary for imaging in more than one dimension;

(2) multipulse techniques wherein the gradient-induced spatial information is encoded to produce frequencies in the decay envelope whose periods are long in comparison with the multipulse cycle time; the technology is complex and instrumentation requirements are sophisticated;

(3) multiple spin-echo methods combined with RF pulse methods that extend T_2 and in which the spatial information is encoded on the actual echo envelope; the equivalent narrow frequency bandwidth is achieved by addition of the echo signals to average out the noise.

Imaging for the purpose of studying materials does not usually have the same premium on the time required to obtain an acceptable image as medical applications. However, the ultimate resolution and sensitivity is determined by the size of the gradient, which determines spectrometer bandwidth requirements and hence the signal-to-noise. Sensitivity and therefore resolution can usually be increased by noise-averaging techniques but there is always a practical limit on the time available for any measurement. It is therefore very important to consider the timescale of data collection. This means that methods such as 'fixed-time' observation with variable field gradient as proposed by Emid & Creyghton (1985) and developed to greater sophistication by McDonald *et al.* (1987) with the use of solid echoes, as well as the sensitive point methods, are at a disadvantage. The multipulse methods are capable of narrow bandwidth filter procedures whereas the direct large field gradient methods require a very large bandwidth. Both multipulse line-narrowing and extended echo sequences achieve, in principle, a significant gain in 'information gathered per unit time' and hence they gain potential sensitivity and resolution.

It is important to remember that in multipulse line-narrowing experiments that use complex pulse cycles (MREV-8, etc.) the signal is only available for observation in certain windows during each pulse cycle. As discussed by Miller & Garroway (1989), the gain in signal-to-noise achieved by line-narrowing may be largely counter-balanced by the noise filter requirements set by the observable fraction, f, within a cycle. This is often less than 10%. Thus the gain in signal-to-noise ratio due to the increased transverse decay time T_2^+ is reduced giving an actual enhancement of $(fT_2^+/T_2)^{\frac{1}{2}}$. In broad-line imaging $f = 1$ but $T_2^+ = T_2$. With the sustained gradient echo modulation method again $f = 1$ but $T_2^+ \gg T_2$. There would appear to be a potential gain of about $\sqrt{10}$ by the latter method over the multipulse narrowing methods and line narrowing efficiency of these methods needs to be $1/f$ times greater to be comparable. For 'intermediate' materials with molecular motion occurring at frequencies comparable to the cycle frequency the response to multipulse line-narrowing can be impaired. The sustained gradient echoes seem less sensitive to this problem.

The actual design of the RF system needed for the gradient echo modulation methods has more severe bandwidth requirements than the multipulse method. This is because gradient modulation is observed between the RF pulse in the former method but only amplitude measurement on this timescale is required for the latter. Also, much larger field gradients are necessary (increased by T_2/T_2^+), which creates a power dissipation problem, particularly if larger objects are to be imaged. This can be off-set by using gradients with a sinusoidal time dependence and tuned gradient coils, but there is a cost involved since nonlinear sampling is required. Both the wide-line gradient echo modulation and multipulse line-narrowing methods are technically demanding. The former is perhaps more suited to small-scale imaging. It also has the (apparently unique) advantage of two-dimensional solid state imaging capability in

PHILOSOPHICAL TRANSACTIONS OF THE ROYAL SOCIETY A MATHEMATICAL, PHYSICAL & ENGINEERING SCIENCES

a time T_2^+ and is basically simpler to implement. Even unsustained echo experiments have shown that T_1 and T_2 mapping in small-scale solid samples is a practical proposition and that it can be used to non-destructively study the structural nature and change of solid materials. Sustained echo methods or multipulse narrowing with a high quality spectrometer should open up many opportunities for materials investigation.

The author thanks Dr S. P. Cottrell, Dr M. R. Halse and Dr P. J. McDonald for useful discussions and Dr Miller and Dr Garroway for providing preprints of their work before publication.

References

Brooks, R. A. & Di Chiro, G. 1975 *Radiology* **117**, 56–572.

Carpenter, T. A., Hall, L. D. & Jezzard, P. 1989 *J. magn. Reson.* **84**, 383–387.

Chingas, G. C., Miller, J. B. & Garroway, A. N. 1986 *J. magn. Reson.* **66**, 530–535.

Corti, M., Borsa, F. & Rigamonti, A. 1988 *J. magn. Reson.* **79**, 21–27.

Cory, D. G., Reichwein, A. M., Van Os, J. W. M. & Veeman, W. S. 1988 *Chem. Phys. Lett.* **143**, 467–470.

Cory, D. G., Miller, J. B. & Garroway, A. N. 1990 *Molec. Phys.* **70**, 331–345.

Cottrell, S. P. 1990 Ph.D. thesis, University of Kent, U.K.

Cottrell, S. P., Halse, M. R., Ibbett, D. A. & Strange, J. H. 1990 (In the press.)

Cottrell, S. P., Halse, M. R., McDonald, P. J., Strange, J. H. & Tokarczuk, P. F. 1989 *Bull. magn. Reson.* 310–313.

Cottrell, S. P., Halse, M. R. & Strange, J. H. 1990 *Meas. Sci. Technol.* **1**, 624–629.

Cottrell, S. P., Ibbett, D. A., Halse, M. R. & Strange, J. H. 1988 *Proceedings of the Ampere Summer School and Symposium, Magnetic resonance and relaxation: new fields and techniques* (ed. R. Blinc, M. Vilfan & J. Slak), Ljubljana, pp. 61–62.

Emid, S. & Creyghton, J. H. N. 1985 *Phys.* B **128**, 81–83.

Garroway, A. N., Baum, J., Munowitz, M. G. & Pines, A. 1984 *J. magn. Reson.* **60**, 337–341.

Hahn, E. L. 1950 *Phys. Rev.* **80**, 580–594.

Halse, M. R., Mat Daud, Y., Rahman, H. & Strange, J. H. 1990 (In the press.)

Ibbett, D. A. 1988 Ph.D. thesis, University of Kent, U.K.

Kumar, A., Welti, D. & Ernst, R. R. 1975 *Naturwissenschaft* **62**, 34.

Lai, C. M. & Lauterbur, P. C. 1980 *J. Phys.* E **13**, 747–751.

Mansfield, P. & Grannell, P. K. 1973 *J. Phys.* C **6**, L422–426.

Mansfield, P. & Grannell, P. K. 1975 *Phys. Rev.* B **12**, 3618–3634.

Mansfield, P. & Ware, D. 1966 *Phys. Lett.* **22**, 133–135.

Mansfield, P. 1971 *J. Phys.* C **4**, 1444–1452.

Mansfield, P. 1977 *J. Phys.* C **10**, L55–58.

McDonald, P. J. & Tokarczuk, P. F. 1989 *J. Phys.* E **22**, 948–951.

McDonald, P. J., Attard, J. J. & Taylor, D. J. 1987 *J. magn. Reson.* **72**, 224–229.

Meiboom, S. & Gill, S. 1958 *Rev. Sci. Instrum.* **29**, 688–691.

Miller, J. B. & Garroway, A. N. 1989 *J. magn. Reson.* **82**, 529–538.

Miller, J. B., Cory, D. G. & Garroway, A. N. 1989 *Chem. Phys. Lett.* **164**, 1–4.

Ordidge, R. J. & Mansfield, P. 1985 U.S. Patent no. 4 509 015.

Ostroff, E. D. & Waugh, J. S. 1966 *Phys. Rev. Lett.* **16**, 1097–1098.

Samoylenko, A. A. Yu., Artemov, D. & Sibeldina, L. A. 1987 *Bruker Rep.* **2**, 30.

Samoylenko, A. A. Yu., Artemov, D. & Sibeldina, L. A. 1988 *JETP Lett.* **47**, 348–350.

Suits, B. H. & White, D. 1984 *Solid St. Commun.* **50**, 291–295.

Wind, R. A. & Yannoni, C. S. 1979 *J. magn. Reson.* **36**, 269–272.

PHILOSOPHICAL TRANSACTIONS OF THE ROYAL SOCIETY A MATHEMATICAL, PHYSICAL & ENGINEERING SCIENCES

Discussion

P. Mansfield (*University of Nottingham, U.K.*). Professor Strange has concentrated on looking at the solid matrix in polymer systems and of course polymers are porous and can absorb fluids like water and also contain plastic pockets. His technique can in principle image both solid and liquid regions and therefore gives a total view. Is there potential for combining the relaxation and diffusion approaches being used by Professor Packer where he is looking at liquids in a solid non-resonant matrix with a knowledge of the solid matrix itself in these polymers?

J. H. Strange. This is a most interesting suggestion. Spatial distribution of relaxation, dependence of relaxation on absorbate density in pores, rate of pore filling, etc., could all be investigated at the same time as the measurement of any changes brought about in the absorbing matrix. Some polymers, such as rubbers, can undergo swelling in which volume changes are enormous. Such processes could be studied in detail from both absorbent and absorbate points of view. Another point is that absorbed liquids in fine pores often exhibit broad NMR lines so that our methods would be very valuable in that case.

M. Wormald (*Oxford University, U.K.*). The distortions of images by susceptibility heterogeneities depend on G (gradient), whereas relaxation depends on G^2. Therefore the distortions are generally longer range. The PbF_2/SnF_2 system will produce a magnetic susceptibility discontinuity and thus change the field gradients present which may result in intensity distortions.

J. H. Strange. Magnetic susceptibility discontinuities can certainly cause major distortions in liquid-state imaging. Unless susceptibility changes are very large indeed they are unlikely to produce a problem in our 'big-gradient' methods although they could possibly prove troublesome with multipulse methods.

W. Derbyshire (*RHM Research, U.K.*). This is a question related to the observation that if the B_1 field is not large compared with the line width of the solid a modulation of the echo is obtained. Does this modulation convey any useful information, and if so has Professor Strange made any attempts to exploit it?

J. H. Strange. The modulation frequency depends inversely on the 90–180° pulse separation and the depth of modulation depends on the relative magnitude of the linewidth and RF field strength. We have simulated the observed effects but have not yet found any useful way to exploit them.

E. R. Andrew (*University of Florida, U.S.A.*). How large were the peak gradients Professor Strange used in this work and how large was the peak power necessary to generate them?

J. H. Strange. The peak magnetic gradients we have used so far have been 150 G cm^{-1} (1.5 T m^{-1}) and these were generated with 250 W audio amplifiers. The gradient coils used are small and samples in them are limited to about 1 cm diameter.

PHILOSOPHICAL TRANSACTIONS OF THE ROYAL SOCIETY A MATHEMATICAL, PHYSICAL & ENGINEERING SCIENCES

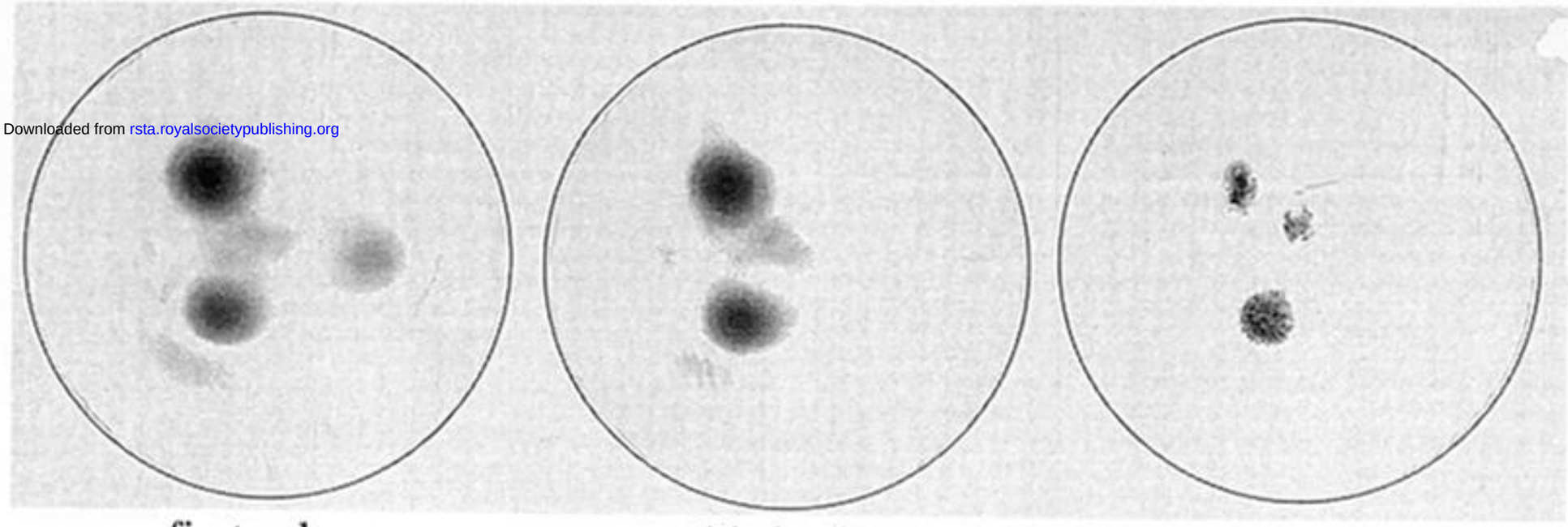

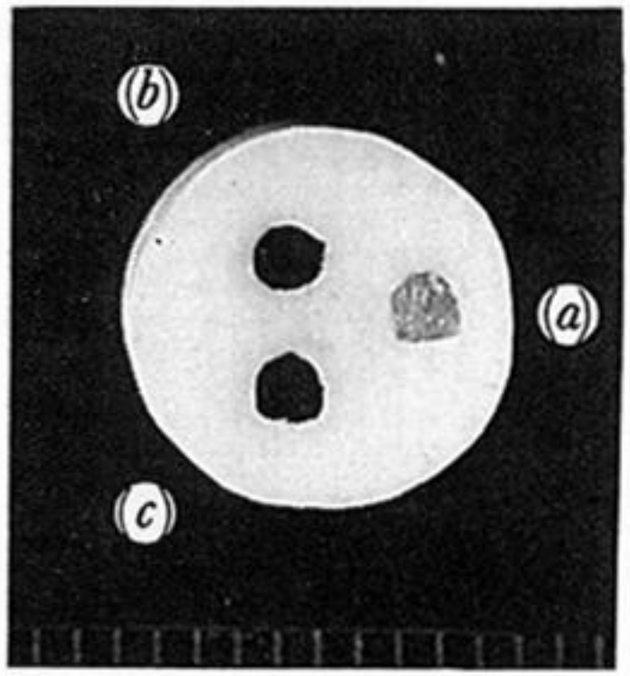

sample

gure 4. Image of three different rubber samples whose T_2s differ due to variation in cross-link ensity. Samples were 1 mm diameter, 3 mm in length. The first, third and ninth echoes occurring $t = 170$ µs, 500 µs and 1.5 ms respectively show the decreased intensity and disappearance of the gnal from the heavily cross-linked sample (a) with $T_2 = 300$ µs and the decreased intensity of mple (b) $T_2 = 750$ µs, relative to sample (c) $T_2 = 900$ µs.

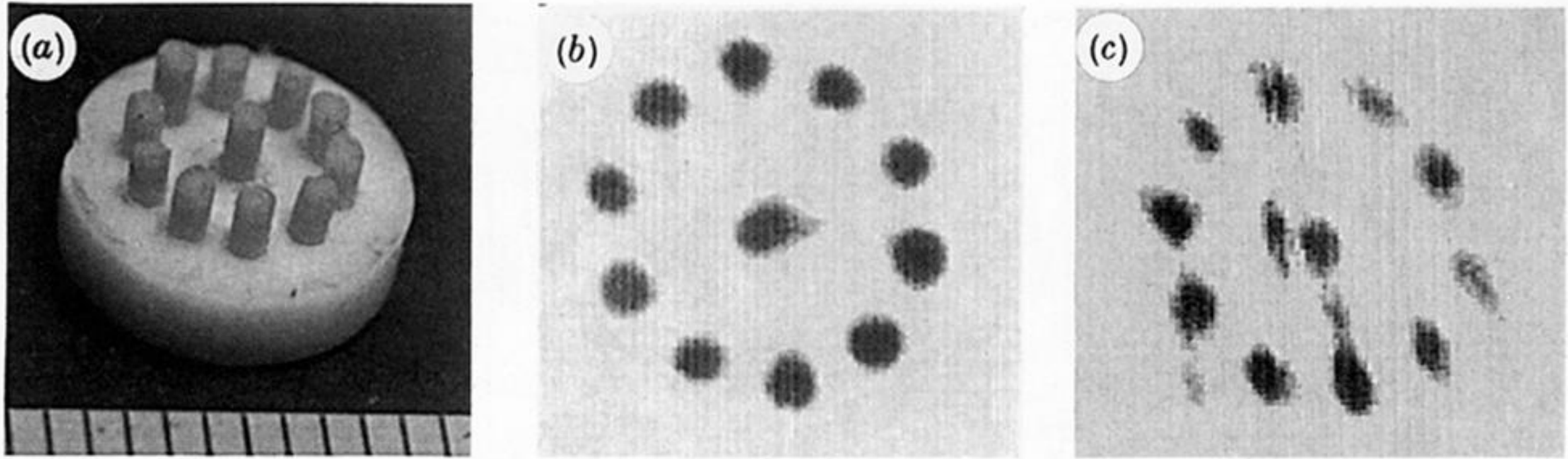

Figure 7. Proton images of the object shown (*a*) on the left were obtained by the spin-echo ethod (*b*) (centre) and the planar method (shown at (*c*) on the right) as described in the text.

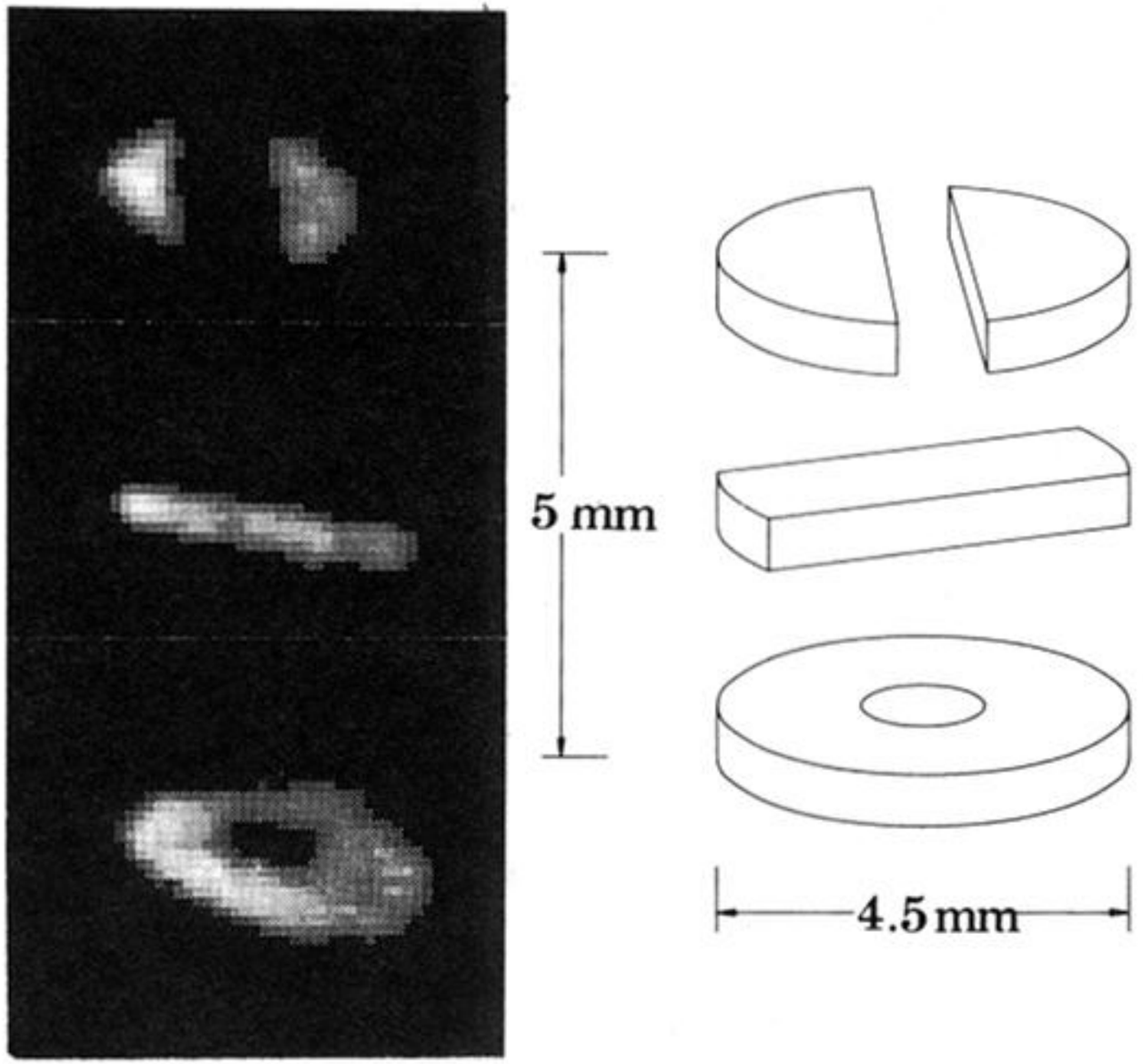

Figure 9. Cross sections obtained by proton imaging in three dimensions of the rubber object shown in the 'exploded' diagram on the right. The three sections were actually in physical contact.